



Walter+Eliza Hall  
Institute of Medical Research

## Institute Research Publication Repository

***This is the author accepted version of :***

Tanzer MC, Tripaydonis A, Webb AI, Young SN, Varghese LN, Hall C, Alexander WS, Hildebrand JM, Silke J, Murphy JM. Necroptosis signalling is tuned by phosphorylation of MLKL residues outside the pseudokinase domain activation loop. *Biochemical Journal*. 2015 471(2):255-265,

***which has been published in final form at***

doi: [10.1042/BJ20150678](https://doi.org/10.1042/BJ20150678).

<http://www.biochemj.org/content/471/2/255.long>

## **Necroptosis signalling is tuned by phosphorylation of MLKL residues outside the pseudokinase domain activation loop**

Maria C. Tanzer<sup>\*,†</sup>, Anne Tripaydonis<sup>\*,†</sup>, Andrew I. Webb<sup>\*,†</sup>, Samuel N. Young<sup>\*</sup>, Leila N. Varghese<sup>\*,†</sup>, Cathrine Hall<sup>\*</sup>, Warren S. Alexander<sup>\*,†</sup>, Joanne M. Hildebrand<sup>†,1</sup>, John Silke<sup>\*,†,1,2</sup>, James M. Murphy<sup>\*,†,1,2</sup>

<sup>\*</sup>The Walter and Eliza Hall Institute of Medical Research, Parkville, Victoria 3052, Australia

<sup>†</sup>Department of Medical Biology, University of Melbourne, Parkville, Victoria 3050, Australia

<sup>1</sup> These authors share senior authorship

<sup>2</sup> To whom correspondence should be addressed: jamesm@wehi.edu.au or silke@wehi.edu.au

**Short title:** MLKL phosphorylation outside the activation loop tunes necroptosis

**Keywords:** Programmed necrosis, pseudoenzyme, cell death, RIPK3, phosphomimetic, four-helix bundle domain

**Summary statement:** We identified phosphorylation sites in MLKL that modulate cell death signalling. Mutations of the MLKL brace region (S158) and pseudokinase N-lobe (S228), and a known site in the activation loop (S345), implicate phosphorylation at these sites in tuning MLKL-mediated necroptosis.

## ABSTRACT

The pseudokinase, MLKL (mixed lineage kinase domain-like), has recently emerged as a critical component of the necroptosis cell death pathway. While it is clear that phosphorylation of the activation loop in the MLKL pseudokinase domain by the upstream protein kinase, RIPK3 (receptor interacting protein kinase-3), is crucial to trigger MLKL activation, it has remained unclear whether other phosphorylation events modulate MLKL function. By reconstituting *Mlkl*<sup>-/-</sup>, *Ripk3*<sup>-/-</sup> and *Mlkl*<sup>-/-</sup>*Ripk3*<sup>-/-</sup> cells with MLKL phospho-site mutants, we compared the function of known MLKL phosphorylation sites in regulating necroptosis with three phospho-sites that we identified by mass spectrometry, S158, S228 and S248. Expression of a phospho-mimetic S345D MLKL activation loop mutant induced stimulus-independent cell death in all knockout cells, demonstrating that RIPK3 phosphorylation of the activation loop of MLKL is sufficient to induce cell death. Cell death was also induced by S228A, S228E and S158A MLKL mutants in the absence of death stimuli, but was most profound in *Mlkl*<sup>-/-</sup>*Ripk3*<sup>-/-</sup> double knockout fibroblasts. These data reveal a potential role for RIPK3 as a suppressor of MLKL activation and indicate that phosphorylation can fine-tune the ability of MLKL to induce necroptosis.

## INTRODUCTION

Necroptosis is a form of cell death that occurs downstream of TNF (Tumour Necrosis Factor) receptor 1 or TLR (Toll-Like Receptor) activation, which is complementary to apoptosis, the prototypical cell death pathway [1]. Unlike apoptosis, which is considered to be immunologically inert, necroptosis is widely thought to elicit inflammatory responses [2-8] and, consequently, has been implicated in the pathogenesis of many diseases, including sepsis, arthritis and pancreatitis [9-11]. Details of the necroptosis pathway are still emerging, with only the protein kinase, receptor interacting protein kinase 3 (RIPK3) [10, 12-14], and the pseudokinase, mixed lineage kinase domain-like (MLKL) [9, 15-17], known to be obligate effectors of the pathway downstream of TNF receptor activation. Necroptotic cell death arises following RIPK3 activation by autophosphorylation and RIPK3-mediated phosphorylation of the pseudokinase domain of MLKL [15-17]. Based on our earlier structural and biochemical analyses, we proposed a molecular switch mechanism [17-19], whereby phosphorylation of the MLKL pseudokinase domain induces a conformational change that leads to unleashing of the N-terminal four-helix bundle (4HB) domain of MLKL [20], which has been shown by us and others to be the executioner domain [20-22]. The precise details of how the MLKL 4HB domain induces cell death are currently a matter of debate [20-24], but it appears that membrane translocation and oligomerization of MLKL are essential to induction of cell death.

We and others have previously established that RIPK3 phosphorylates the activation loop of the MLKL pseudokinase domain to trigger cell death [15, 17, 25]. Earlier work identified S345, S347 and T349 in the mouse MLKL activation loop as sites of RIPK3-mediated phosphorylation, and expression of the phosphomimetic mutant, S345D, was sufficient to induce cell death in cultured fibroblasts [17]. Another site in human MLKL, corresponding to mouse MLKL S124, was phosphorylated in a cell cycle-dependent manner during the G1- to M-phase transition [26, 27]. Here, we used mass spectrometry to identify three further sites of phosphorylation in MLKL: S158, S228 and S248. We examined the role of phosphorylation at each of these five sites in regulating necroptotic death by expressing phosphoablating (Ala) or phosphomimetic (Asp/Glu) mutants in wild-type, *Mlkl*<sup>-/-</sup> and previously-unreported *Ripk3*<sup>-/-</sup>*Mlkl*<sup>-/-</sup> dermal fibroblasts. Our findings support the idea that RIPK3 can potently induce necroptosis via phosphorylation of the MLKL activation loop

residue, S345. Remarkably, the presence of endogenous RIPK3 dampened the capacity of MLKL bearing Glu or Ala substitutions at S228 to induce stimulus-independent cell death. While stimulus-independent cell death arising from mutations of MLKL S228 indicate this site is intrinsically involved in MLKL activation, it is notable that S228 resides at the interface with RIPK3 in the earlier reported complex structure between the MLKL pseudokinase domain and RIPK3 kinase domain [28], suggesting this structure may represent a snapshot of RIPK3-mediated suppression of MLKL. Surprisingly, mutation of MLKL S158 to Ala, but not the phosphomimetic Asp, led to stimulus-independent cell death, raising the possibility that S158 phosphorylation might negatively regulate MLKL activity. Further, MLKL mutants that induced death of *Ripk3<sup>-/-</sup>Mlkl<sup>-/-</sup>* fibroblasts in the absence of stimuli were found to translocate to membranes and assemble into high molecular weight complexes by Blue-Native PAGE, demonstrating that RIPK3 is dispensable for events downstream of MLKL phosphorylation. Collectively, these results support the idea that phosphorylation of MLKL at different sites can tune its activity, but that none of these events activates the cell death function of MLKL as potently as RIPK3-mediated activation loop phosphorylation.

## EXPERIMENTAL

### Expression constructs

A synthetic mouse MLKL cDNA encoding residues 1-464 (DNA2.0, CA) was used as a template for oligonucleotide-directed PCR mutagenesis. All oligonucleotides were synthesised by IDT (Singapore or Coralville, IA). Mutant transcripts were restriction digested and ligated into the doxycycline-inducible, puromycin-selectable vector, pF TRE3G PGK puro and insert sequences verified by sequencing (Micromon DNA Sequencing Facility, VIC, Australia), as described previously [17, 20]. From these expression constructs, lentiviral particles were generated in HEK293T cells as described previously, where vector DNA was co-transfected with pVSVg and pCMV  $\Delta$ R8.2 helper plasmids [17, 20].

### Western blot antibodies

Antibodies used for Western blotting were: the rat anti-MLKL 3H1 monoclonal (available as MABC604, EMD Millipore), which detected both mouse and human MLKL; anti-phospho human MLKL (ab187091, Abcam); rabbit anti VDAC1 (AB10527, Millipore); rabbit anti GAPDH (2118, Cell Signalling Technology); rabbit anti-mouse RIPK3 (PSC-2283-c100, Axxora); mouse anti Actin (A-1987, Sigma).

### Cell lines and cell death assays

U937 and HT29 cells were cultured in human tonicity RPMI medium supplemented with 8-10% v/v fetal calf serum (FCS). Cell death assays were carried out in 12 well plates, seeded at  $1 \times 10^5$  cells per well. Cells were treated for the time periods indicated with TNF (100 ng/mL), Smac-mimetic (500 nM) and Q-VD-Oph (10  $\mu$ M), then harvested, stained with propidium iodide (PI; 1  $\mu$ g/mL) and quantified using a BD FACSCalibur flow cytometer. In parallel experiments, cells were lysed in SDS-PAGE loading buffer (126 mM Tris-HCl pH 8, 20% v/v glycerol, 4% w/v SDS, 0.02% w/v Bromophenol blue, 5% v/v 2-mercaptoethanol) and immunoblotted for phosphorylated MLKL, total MLKL and Actin.

The isolation and immortalization of mouse dermal fibroblasts (MDFs) from the dermis of three *Mlkl<sup>-/-</sup>* and three congenic wild-type mice to generate three biologically independent cell lines were described previously [17]. Analogously, we prepared MDFs from the dermis of three *Ripk3<sup>-/-</sup>Mlkl<sup>-/-</sup>* mice and immortalized these cells by SV40 large T antigen expression. The *Ripk3<sup>-/-</sup>Mlkl<sup>-/-</sup>* mouse strain was generated by intercrossing *Ripk3<sup>-/-</sup>* [29] (kindly provided by Dr Vishva Dixit) and *Mlkl<sup>-/-</sup>* [17] mouse strains, both of which are

maintained on a C57BL/6 genetic background. Haematopoietic analyses were performed as before [17]; blood from 8-12 week old mice was collected into tubes containing EDTA (Sarstedt) and analysed with an Advia 120 analyzer (Bayer). MDFs and HEK293T were maintained in Dulbecco's modified Eagle's medium (DMEM) supplemented with 8-10 % v/v FCS, and puromycin (5 µg/mL) for lines stably transduced with MLKL expression constructs. Cell death assays were carried out in 24 well plates, seeded at  $5 \times 10^4$  cells per well. Cells attached over 4 hours in the presence of 10 ng/mL doxycycline were either untreated or treated with TNF and Smac mimetic, or the TNF, Smac-mimetic and Q-VD-Oph cocktail, as for U937 cells above. Quantitation of cell death was performed as for U937 cells, but 24 hours post-stimulation.

### **Statistical analyses**

Error bars represent Mean  $\pm$  SEM of specified number of independent and/or biological repeats, not technical replicates.

### **Fractionation and Blue Native PAGE**

Fractionation of cells into cytoplasmic and membrane fractions was performed as described previously [20]. Briefly, wild-type U937 or MDF cells were stimulated with TSQ, or MDFs stably transduced with mutant MLKL constructs were induced with 10 ng/mL doxycycline for 7.5 hours, before cells were harvested and permeabilized in buffer (20 mM HEPES pH 7.5, 100 mM KCl, 2.5 mM MgCl<sub>2</sub>, and 100 mM sucrose) containing 0.025% digitonin (BIOSYNTH, Staad, Switzerland), 2 µM N-ethyl maleimide, phosphatase and protease inhibitors. Crude membrane and cytoplasmic fractions were separated by centrifugation (5 min at 11000 g), and the respective fractions prepared in buffers to a final concentration of 1% w/v digitonin. Samples were resolved on a 4-16% Bis-Tris Native PAGE gel, transferred to PVDF for Western blot analyses.

### **Mass spectrometry and data analysis**

Recombinant GST-mRIPK3 (residues 2-353; 1 µg) was incubated for 90 min at 20°C with recombinant mouse MLKL pseudokinase domain (residues 179-464; 5 µg) in kinase reaction buffer (100 mM NaCl, 20 mM Tris pH 8, 4 mM MgCl<sub>2</sub>, 0.1 mM DTT, 0.1 mg/mL BSA) supplemented with 1mM ATP. Both GST-mRIPK3 and mMLKL(179-464) were expressed and purified from Sf21 insect cells according to established procedures [17, 25]. Reactions were terminated by addition of reducing loading buffer and boiling for 5 min, before resolution by 4-20% Tris-Glycine SDS-PAGE (Biorad). Following staining with SYPRO Ruby, MLKL(179-464) bands were excised, in-gel reduced, alkylated and trypsin digested, before analysis by nanoflow reversed-phase liquid chromatography tandem mass spectrometry (LC-MS/MS) on a nanoAcquity system (Waters, Milford, MA, USA) coupled either to a LTQ XL Orbitrap or a Q-Exactive mass spectrometer equipped with a nanoelectrospray ion source for automated MS/MS (Thermo Fisher Scientific, Bremen, Germany), as described previously [20].

$25 \times 10^6$  stably transduced wild-type MDF cells were induced to express exogenous wild-type MLKL bearing a C-terminal StrepII tag for 4 hours with 10 ng/mL doxycycline. Notably, we observed that C-terminal fusion of wild-type full length MLKL to a StrepII tag led to stimulus-independent death (unpublished observations). Cells were lysed in 5 mL ice-cold DISC buffer [30], debris eliminated by centrifugation and supernatant incubated with StrepTactin resin (1 mg) for 1 hour with rotation at 4°C. Beads were washed four times with DISC buffer before elution with three treatments of 50 µL 5 mM biotin. Eluates were processed with trypsin using the filter-aided sample preparation (FASP) protocol, as per published procedures [31], before sample processing and acquisition of mass spectra as

described above. Raw files consisting of high- and low-resolution MS/MS spectra were processed with MaxQuant (version 1.5.2.8) for feature detection and protein identification using the Andromeda search engine [32]. Extracted peak lists were searched against the UniProtKB/Swiss-Prot *Mus musculus* database and a separate reverse decoy database to empirically assess the false discovery rate (FDR) using strict trypsin specificity allowing up to 3 missed cleavages. The minimum required peptide length was set to 6 amino acids. Carbamidomethylation of Cys was set as a fixed modification, while N-acetylation of proteins, oxidation of Met, the addition of pyroglutamate (at N-termini Glu and Gln), phosphorylation (Ser, Thr and Tyr), deamidation (Asn, Gln and Arg), were set as variable modifications. The mass tolerance for precursor ions was set at 5 ppm and fragment ions 10 ppm and 0.5 Da (Q-Exactive and Orbitrap XL respectively).

## RESULTS

### **MLKL activation loop phosphorylation and membrane localization precedes cell death**

In order to investigate the relationship between MLKL phosphorylation, its membrane association and cell death, we examined necroptosis in the human histiocytic lymphoma cell line, U937. We chose to monitor MLKL phosphorylation, death and membrane translocation using human cells, because, until very recently, only phospho-human MLKL antibodies were commercially available [23]. The 3H1 total MLKL antibody that we previously described [17], on the other hand, readily detected both human and mouse MLKL (Figure 1A and C). We induced necroptosis in U937 cells using conventional necroptotic stimuli: tumour necrosis factor (TNF; T), to activate TNF receptor 1 signalling; the Smac-mimetic, Compound A (S), to inhibit cIAP-mediated ubiquitylation of RIPK1 and allow its participation in cell death pathways; and the pan-caspase inhibitor, Q-VD-OPh (Q), to inhibit caspase-driven apoptotic signalling. We readily detected MLKL phosphorylation at T357/S158 6 hours following TSQ stimulation in U937 cells (Figure 1A). Phosphorylated MLKL was still present 24 hours after stimulation although, owing to cell death induced by TSQ, total protein levels and correspondingly, MLKL levels, were reduced. In parallel, we monitored cell death by measuring uptake of the DNA-binding dye, propidium iodide (PI), by flow cytometry. The majority of cell death occurred within 24 hours, but very little cell death was observed at 3, 6 and 10 hours (Figure 1B). This was surprising because MLKL phosphorylation was readily and reproducibly observed by 6 hours post-TSQ stimulation (Figure 1A). This delay was not unique to U937 cells, because we observed the same discrepancy between phosphorylation onset and detectable cell death in another human cell line commonly used for necroptosis studies, HT29 (Figure 1C and D).

This led us to examine whether phosphorylated MLKL immediately translocated to the plasma membrane or whether a delay in phospho-MLKL membrane translocation accounted for the lag in cell death. We therefore fractionated cells into cytoplasmic and total membrane preparations, before resolving proteins by Blue-Native PAGE and examining the localization of MLKL by Western blot (Figure 1E). MLKL translocation and incorporation into high molecular complexes in the membrane fraction was coincident with phosphorylation of its activation loop rather than cell death. These data are consistent with the idea that activation loop phosphorylation is not the sole cue for MLKL to mediate cell death, but rather that other modifications or signalling events are required. Coupled with a broader interest in understanding how MLKL activity can be tuned by phosphorylation, we proceeded to examine whether other phosphorylation events extraneous to the activation loop contribute to MLKL-mediated cell death.

### Identification of three phosphorylation sites in mouse MLKL by mass spectrometry

We sought to identify phosphorylation sites, in addition to the previously reported activation loop residues in mouse MLKL (S345, S347, T349) [17, 28] that might contribute to regulation of its necroptotic function. We focused on identifying phosphorylation sites in mouse MLKL, because we have previously established a cellular system that allows reconstitution of *Mlkl*-deficient cells with mutant constructs to assess their functions [17, 20]. We used recombinant mouse RIPK3 kinase domain to phosphorylate mouse MLKL pseudokinase domain *in vitro*. In addition to the previously described phosphorylation sites in the activation loop [17], we identified the phosphorylated residues S228 and S248 by mass spectrometry (Figure 2B and C). S228 is located in the N-lobe and S248 in the hinge region of the pseudokinase domain (Figure 2A).

In a complementary experiment, we stably-transduced wild-type mouse dermal fibroblast (MDF) cells with a C-terminally StrepII-tagged murine MLKL construct, which we found induced cell death in the absence of additional stimuli. Following induction of protein expression by addition of 10 ng/mL doxycycline for 4 hours, cells were lysed and StrepII-tagged MLKL enriched with StrepTactin resin. The biotin eluate was processed with trypsin using the FASP protocol, and the resultant peptide sample analysed using high resolution mass spectrometry. This experiment enabled us to identify S158 (Figure 2D), a residue located in the second of the two “brace” helices that connect the 4HB and pseudokinase domains of mouse MLKL (Figure 2A), as a site of MLKL phosphorylation. Notably, no other phosphorylated residues in MLKL were identified in this preparation, and S158 was not detectably phosphorylated by mass spectrometry in experiments in which recombinant MLKL was phosphorylated by RIPK3.

### Differential effects of phosphomimetic and phosphoablating mutations on necroptosis induction by MLKL

To analyse the impact on necroptotic activity of phosphorylation at individual serine residues within MLKL, we generated doxycycline-inducible expression constructs of murine MLKL with mutations that mimic (negatively-charged Asp or Glu residues), or prevent (Ala), serine phosphorylation. In addition to the newly discovered S158, S228 and S248 phosphosites, we mutated previously reported phosphorylated residues, S345 and S124, for comparison. Our earlier work established that substitution of S345 in the MLKL pseudokinase domain activation loop with the phosphomimetic, Asp, potently induced necroptosis [17]. In contrast, phosphorylation of S125 in the 4HB domain of human MLKL was previously reported to occur in a cell cycle dependent manner [26, 27], but how this impacts MLKL function has not been assessed. Here, we prepared phosphomimetic (Glu) or phosphoablating (Ala) mutations of the orthologous residue in mouse MLKL, S124, to examine its function in necroptosis signalling.

Wild-type and *Mlkl*<sup>-/-</sup> MDF cells were stably-transduced with lentiviruses encoding doxycycline-inducible MLKL constructs, were either induced or not, then left untreated (UT) or stimulated with apoptotic (TS) or necroptotic (TSQ) stimuli for 24 hours before cell death was detected by propidium iodide-staining and quantified by flow cytometry. Expression of MLKL mutants in wild-type cells, with endogenous MLKL, allowed us to determine whether the mutants affected endogenous necroptosis signalling, whereas expression in *Mlkl*<sup>-/-</sup> cells allowed us to examine whether these MLKL mutants were able to reconstitute the necroptosis pathway. Only modest levels of cell death (20-25%) were observed in three biologically independent control wild-type and *Mlkl*<sup>-/-</sup> MDF cell lines expressing exogenous wild-type MLKL unless they were stimulated with either TS or TSQ (Figure 3A). In contrast, but consistent with our earlier report [17], expression of S345D MLKL in wild-type MDF cells induced profound cell death (~70%) in the absence of any other treatment (Figure 3B).

Using the same approach, we tested whether our phosphosite Ala and Glu/Asp MLKL mutants induced cell death in the absence of any stimulus, as well as in the presence of apoptosis (TS) and necroptosis (TSQ) stimuli. All mutants were expressed at similar levels in three biologically independent wild type and MLKL knock-out MDF cell lines and to the same levels as wild type MLKL (Supplementary Figure 1). This indicated that mutation of these residues did not affect MLKL folding or stability. Notably, all mutants, except S248E MLKL, restored the susceptibility of *Mlkl*<sup>-/-</sup> cells to TSQ-induced necroptosis to the same levels as wild type MLKL (Figure 3F). Expression of either S228A, S248A or S124A MLKL induced only modest death when expressed in wild-type and *Mlkl*<sup>-/-</sup> cells in the absence of death stimuli (Figure 3C, E and G), and this was only marginally more death than that observed in control cells reconstituted with wild-type MLKL (Figure 3A). In contrast, phosphomimetic Asp/Glu substitutions of these residues had varying effects. Expression of S228E MLKL, in the absence of other stimuli, induced ~40% cell death in either wild-type or *Mlkl*<sup>-/-</sup> cells (Figure 3D), while S248E (Figure 3F) and S124E MLKL (Figure 3H) induced minimal death, comparable to wild-type MLKL (Figure 3A). Interestingly, expression of S158A MLKL was a relatively potent inducer of cell death in the absence of other stimuli in both wild-type and *Mlkl*<sup>-/-</sup> cells with ~50% death observed (Figure 3I). In comparison, expression of S158D MLKL induced modest cell death in both wild-type and *Mlkl*<sup>-/-</sup> cells in the absence of death stimuli (Figure 3J), comparable to that observed in cells expressing wild-type MLKL (Figure 3A).

#### **Activated MLKL mutants cause necroptosis in the absence of RIPK3 and MLKL**

RIPK3 has been reported to directly engage MLKL and mediate its recruitment to the necrosome following induction of necroptosis [15, 16]. RIPK3-mediated phosphorylation of MLKL at S345 in the pseudokinase domain activation loop has been assumed to be the crucial, and sufficient, step to trigger MLKL activation. MLKL phosphorylation is presumed to induce translocation to biological membranes and consequent cell death. However, it is currently unclear whether RIPK3 might regulate MLKL in other ways besides mediating its phosphorylation. To investigate this, we expressed our collection of mutant MLKL constructs in fibroblast cell lines derived from the dermis of *Ripk3*<sup>-/-</sup>*Mlkl*<sup>-/-</sup> mice. The *Ripk3*<sup>-/-</sup>*Mlkl*<sup>-/-</sup> mice resembled *Ripk3*<sup>-/-</sup> and *Mlkl*<sup>-/-</sup> single knockout mice, which were similarly viable and fertile, with no overt pathology under stress-free conditions. Haematological analyses of 8-12 week old *Ripk3*<sup>-/-</sup>*Mlkl*<sup>-/-</sup> animals revealed no significant abnormalities in their blood cell populations relative to wild-type, *Mlkl*<sup>-/-</sup> and *Ripk3*<sup>-/-</sup> animals (Supplementary Table 1), except for a statistically significant decrease (P<0.05) in circulating monocytes relative to *Mlkl*<sup>-/-</sup> mice and statistically significant (P<0.05) increases in lymphocytes and eosinophils in male mice relative to their *Mlkl*<sup>-/-</sup> and *Ripk3*<sup>-/-</sup> counterparts, respectively. We confirmed the absence of MLKL and RIPK3 in these cells by Western blot of whole cell lysates (Figure 4A). As expected, *Ripk3*<sup>-/-</sup>*Mlkl*<sup>-/-</sup> MDFs were, like *Ripk3*<sup>-/-</sup> and *Mlkl*<sup>-/-</sup> cells, completely protected from TSQ-induced necroptosis (Figure 4B) and expression of wild-type MLKL in the *Ripk3*<sup>-/-</sup>*Mlkl*<sup>-/-</sup> MDFs failed to restore susceptibility to TSQ-induced necroptosis (Figure 4C). However, expression of S345D MLKL, a mutation that mimics phosphorylation of the MLKL activation loop by RIPK3, was sufficient to induce cell death in the absence of any stimulus (Figure 4D). These observations support the hypothesis that phosphorylation of the MLKL activation loop is the principal function of RIPK3 in necroptosis signalling.

We sought to establish the functions of other MLKL phosphosites in the absence of endogenous RIPK3 and MLKL by expressing MLKL mutants bearing Ala and Glu/Asp substitutions at S124, S158, S228 and S248 to ablate or mimic phosphorylation, respectively (Figure 4E-L). Interestingly, expression of the MLKL Ala mutants in double knockout cells induced measurable cell death, markedly higher than that observed when the same mutants

were expressed in wild-type or *Mlkl*<sup>-/-</sup> cells (Figure 3). S228A and S158A MLKL induced ~60% cell death, and S248A and S124A MLKL ~40%, when expressed in *Ripk3*<sup>-/-</sup>*Mlkl*<sup>-/-</sup> MDFs. In contrast, mirroring our observations in wild-type and *Mlkl*<sup>-/-</sup> MDFs (Figure 3), S248E, S124E and S158D MLKL, each had negligible impact on *Ripk3*<sup>-/-</sup>*Mlkl*<sup>-/-</sup> cell viability (Figure 4F, H, J, L). S228E MLKL, on the other hand, potently induced death of *Ripk3*<sup>-/-</sup>*Mlkl*<sup>-/-</sup> cells, with ~70% death observed (Figure 4F). This level of death was higher than when expressed in wild-type (~50% death) or *Mlkl*<sup>-/-</sup> (~40% death) MDF cells (Figure 3D). Because these residues were phosphorylated by RIPK3 *in vitro*, the elevated death observed when the S228A and S228E MLKL mutants were expressed in *Ripk3*<sup>-/-</sup>*Mlkl*<sup>-/-</sup> cells suggests a potential role for RIPK3 in suppressing activation of these mutants in wild-type and *Mlkl*<sup>-/-</sup> cells.

### **Activated MLKL mutants assemble into membrane bound oligomers in the absence of necroptotic stimulation**

Upon activation, MLKL translocates from the cytoplasm to biological membranes where it is incorporated into the high molecular weight complexes that mediate cell death [20-24]. As shown previously ([20] and Figure 1E), incorporation of MLKL into these high molecular weight complexes can be monitored by Blue-Native PAGE. Here, we compared the membrane translocation of endogenous MLKL in wild-type MDF cells treated with TSQ with that of the induced expression of activated S345D MLKL in wild-type, *Mlkl*<sup>-/-</sup> and *Ripk3*<sup>-/-</sup>*Mlkl*<sup>-/-</sup> cells (Figure 5A). In untreated wild-type cells, MLKL was exclusively cytoplasmic and ran at a position in a Blue-Native gel between the 66 and 146 kDa molecular weight markers (Figure 5A). As expected, TSQ-treatment of wild-type MDF cells led to membrane translocation and assembly into higher molecular weight complexes (~480 kDa, [20]). In contrast, in each of the wild-type, *Mlkl*<sup>-/-</sup> and *Ripk3*<sup>-/-</sup>*Mlkl*<sup>-/-</sup> cells, a fraction of activated S345D MLKL mutant was present in the membrane compartment as a higher molecular weight form within 7.5 hours of induced expression and in the absence of a necroptotic stimulus (Figure 5A). A similar phenomenon was observed upon expression of the activated MLKL mutants identified in this study, S228A, S228E, S158A, and to a lesser extent, S248A, in *Ripk3*<sup>-/-</sup>*Mlkl*<sup>-/-</sup> MDF cells (Figure 5B,C). We observed translocation of the activated MLKL mutants from the cytoplasm to form a high molecular weight complex in the membrane fraction. Notably, this high molecular weight complex was not observed in cells expressing the S124E and S248E MLKL mutants (Figure 5B,C), consistent with the negligible cell death induced by these mutants. Surprisingly, S158D and S124A MLKL, two mutants that induced only negligible cell death, translocated to the membrane fraction and assembled into high molecular weight complexes (Figure 5C), suggesting that mutation of these residues promotes membrane translocation but perturbs some downstream signalling event necessary to induce necroptosis. Overall, these data indicate that formation of a RIPK3:MLKL complex is not required to mediate membrane translocation.

## **DISCUSSION**

Because of its essential role in signalling for necroptotic cell death, the precise choreography of MLKL activation is of immense interest. To date, only RIPK3-mediated phosphorylation of residues in the activation loop of MLKL's pseudokinase domain has been established as an essential step in the induction of necroptosis [15, 17, 23, 33] and it is believed that this results in a conformational change in MLKL that is sufficient to unleash the membrane permeabilising function of the MLKL 4-Helical Bundle (4HB) [20]. Consistent with this model of MLKL activation, expression of a phosphomimetic S345D mutant MLKL in MLKL deficient cells induced necroptosis [17], and Rodriguez *et al.* [33] concluded that RIPK3-

mediated phosphorylation of MLKL at S345 was the key step in MLKL activation, while phosphorylation of the neighbouring, S347 and T349, played only auxiliary or negligible roles, respectively, in necroptotic death. We were surprised therefore to observe that phosphorylation of the activation loop preceded cell death by several hours. This suggested that additional points of regulation of MLKL's killing activity exist. We hypothesised that phosphorylation at other sites in MLKL might regulate its activation and subsequent necroptosis. We therefore identified additional residues in MLKL that were phosphorylated and generated Glu/Asp (phospho-mimetic) or Ala (phospho-ablating) mutants of these and tested their ability to induce cell death on their own or following a necroptosis stimulus. Of the four additional sites S124 is the mouse counterpart of a known human MLKL phosphosite, and S158, S228 and S248 were phosphosites identified by mass spectrometry in this study. Like S345, S228 and S248 were identified as sites in MLKL that are subject to RIPK3-mediated phosphorylation, while S124 and S158 were not phosphorylated by RIPK3 *in vitro* and the identities of the responsible kinases are unknown.

While the functions of MLKL S124, S158, S228 and S248 phosphorylation were unknown, it has been shown that the phospho-mimetic mutation, S345D can cause MLKL activation and constitutive cell death in the absence of stimuli [17]. However it was unknown whether RIPK3 contributed to MLKL induced necroptosis in another way, for example as a co-factor for membrane translocation. The fact that expression of S345D MLKL induced cell death, in *Ripk3<sup>-/-</sup>Mlkl<sup>-/-</sup>* MDFs strongly supports the hypothesis that phosphorylation of the MLKL pseudokinase domain activation loop is the essential and sufficient step in MLKL activation required to cause necroptosis. This conclusion is supported by Rodriguez *et al.* [33], who observed RIPK3-independent membrane translocation and cell death in MEFs expressing S345D MLKL.

Of the other four MLKL phosphorylation sites examined in our study, only the S228E phosphomimetic mutation induced measurable cell death in the absence of stimuli when expressed in wild-type, *Mlkl<sup>-/-</sup>* and *Ripk3<sup>-/-</sup>Mlkl<sup>-/-</sup>* cells. S228E MLKL induced pronounced death of wild-type (~50% death) and *Mlkl<sup>-/-</sup>* MDFs (~40% death), which was exacerbated in *Ripk3<sup>-/-</sup>Mlkl<sup>-/-</sup>* MDFs (~70% death) to a level of death comparable to S345D MLKL. Thus the S228E mutation activated MLKL-mediated cell death and this effect was dampened in cells expressing endogenous RIPK3. S228 resides adjacent to helix  $\alpha$ C in the N-lobe of the MLKL pseudokinase domain (Figure 2A) and, based on the co-crystal structure of the mouse MLKL pseudokinase and RIPK3 kinase domains [28], it has previously been proposed to form part of an interaction interface with RIPK3. Our observations led us to hypothesize that the face-to-face interaction of the RIPK3 kinase domain with the MLKL pseudokinase domain observed in the MLKL:RIPK3 co-crystal structure might have captured a snapshot of an unappreciated function of RIPK3 as a suppressor of MLKL activation. It is, however, also plausible that mutation of S228 could affect the structure of the proximal MLKL activation loop, and in so doing may trigger the molecular switch mechanism to unleash the executioner four-helix bundle domain. Notably, S228A MLKL induced negligible cell death in *Mlkl<sup>-/-</sup>* MDFs. In contrast, expression of S228A MLKL in *Ripk3<sup>-/-</sup>Mlkl<sup>-/-</sup>* MDFs led to ~60% cell death. Together these data imply that modification of S228 intrinsically activates cell death unless RIPK3 is present to act as a suppressor, either directly or indirectly. It is also noteworthy that Ala mutants of S124 and S248 induced ~40% death in *Ripk3<sup>-/-</sup>Mlkl<sup>-/-</sup>* MDFs and, like S228A MLKL, induced negligible death in *Mlkl<sup>-/-</sup>* MDFs. These results suggest that RIPK3 helps suppress MLKL auto-activation, although the underlying mechanism is presently unclear.

Another surprising observation was that mutation of S158, a residue located in the second of the brace helices that connects the 4HB and pseudokinase domains (Figure 2A), induced cell death in wild-type, *Mlkl<sup>-/-</sup>* and *Ripk3<sup>-/-</sup>Mlkl<sup>-/-</sup>* cells when mutated to Ala, a phospho-ablating mutation, while a phospho-mimetic mutant did not activate MLKL in the

same manner. While we cannot exclude the possibility that Ala mutation leads to auto-activation of MLKL because of disruption of suppressive interaction(s) with the MLKL pseudokinase domain or other unidentified regulatory proteins, these data suggest that phosphorylation of S158 may serve a role in suppressing MLKL activation. S158 is conserved in the mouse, rat, horse, cow and platypus MLKL sequences, with proximal sites present in primate sequences that are homologous to human MLKL S161. We anticipate future studies will illuminate whether the proximal site in human MLKL is subject to regulation by phosphorylation and whether this serves a suppressive function in MLKL activation. Based on the fact that we did not observe RIPK3-mediated phosphorylation of S158 *in vitro*, it is likely that a kinase other than RIPK3 is responsible for this modification in cells.

RIPK3 has been reported to directly bind and recruit MLKL to the necrosome where it can be activated by phosphorylation [15, 16], although we have been unable to observe such an interaction between the endogenous proteins [17]. Therefore it is possible that RIPK3 has additional roles beyond activating MLKL via phosphorylation, for example, by directly contributing to membrane translocation of MLKL. To address this possibility we examined the cellular localization and oligomerization of MLKL mutants expressed in *Ripk3<sup>-/-</sup>Mlkl<sup>-/-</sup>* MDFs (Figure 4). Mutants that killed *Ripk3<sup>-/-</sup>Mlkl<sup>-/-</sup>* MDFs (S345D, S158A, S228A, S228E and to a lesser extent S248A) translocated to membrane fractions and assembled into high molecular species, while those that did not kill cells (S124E and S248E) did not, as anticipated. Unexpectedly, S124A and S158D MLKL, two mutants that did not constitutively kill *Ripk3<sup>-/-</sup>Mlkl<sup>-/-</sup>* MDFs, translocated to membrane fractions and assembled into high molecular weight complexes (Figure 5). This finding suggests that the S124A and S158D mutations promote membrane translocation and MLKL oligomerisation, but additional downstream signalling events are required for necroptosis to occur. Additionally, our observations in cells lacking RIPK3 indicate that the principal function of RIPK3 is to phosphorylate MLKL, whether or not this involves recruitment to the necrosome, and that it is dispensable for membrane translocation subsequent to MLKL activation. It remains of enormous interest to deduce why there is disconnection in the kinetics of MLKL phosphorylation/membrane localization and the initiation of cell death (Figure 1). Our analysis of the roles of different MLKL phosphosites using phosphomimetic and phosphoablating mutants is suggestive that phosphorylation at S158 and S228 may respectively suppress and enhance MLKL activation to tune the response of a cell to a necroptotic stimulus. While highly suggestive, further validation of this hypothesis in cells will rely on future development of phosphospecific antibodies that detect these phosphorylation events. Furthermore, while phosphorylation events on MLKL are likely to tune its activation potential, the findings presented here do not preclude the possibility that additional effectors are required downstream of MLKL activation to induce cell death, with a number of candidates already proposed in various cellular settings [22, 24].

## **ACKNOWLEDGMENTS**

We thank Dr Vishva Dixit for kind provision of the *Ripk3*<sup>-/-</sup> mice; Prof. Mark Hampton and Dr Andreas Konigstorfer for HT29 cells; Bioservices staff at the Walter and Eliza Hall Institute for assistance with animal handling; Doreen Agyapomaa for mass spectrometry sample processing; Dr Toru Okamoto for developing the inducible expression vectors; and Jason Corbin, Jasmine McManus and Annette Jacobsen for technical assistance.

## **AUTHOR CONTRIBUTIONS**

MCT, JMH, JS and JMM designed the study; MCT, AT, AIW, SNY, LNV, CH, WSA, JMH and JMM performed experiments; MCT, AT, AIW, WSA, JMH, JS and JMM analysed results; MCT, JS, JMM wrote the paper with input from all authors.

## **FUNDING**

This work was supported by National Health and Medical Research Council of Australia (NHMRC) grants (1016647, 1057888, 1057905, 1046010) and fellowships to WSA (1058344), JMH (541951) and JS (541901, 1058190); an Australian Research Council Future Fellowship to JMM (FT100100100); a Victorian International Research Scholarship to M.C.T; with additional support from the Victorian State Government Operational Infrastructure Support, NHMRC IRIISS grant (361646).

## REFERENCES

- 1 Murphy, J. M. and Silke, J. (2014) Ars Moriendi; the art of dying well - new insights into the molecular pathways of necroptotic cell death. *EMBO Rep.* **15**, 155-164
- 2 Rickard, J. A., O'Donnell, J. A., Evans, J. M., Lalaoui, N., Poh, A. R., Rogers, T., Vince, J. E., Lawlor, K. E., Ninnis, R. L., Anderton, H., Hall, C., Spall, S. K., Phesse, T. J., Abud, H. E., Cengia, L. H., Corbin, J., Mifsud, S., Di Rago, L., Metcalf, D., Ernst, M., Dewson, G., Roberts, A. W., Alexander, W. S., Murphy, J. M., Ekert, P. G., Masters, S. L., Vaux, D. L., Croker, B. A., Gerlic, M. and Silke, J. (2014) RIPK1 regulates RIPK3-MLKL-driven systemic inflammation and emergency hematopoiesis. *Cell.* **157**, 1175-1188
- 3 Rickard, J. A., Anderton, H., Etemadi, N., Nachbur, U., Darding, M., Peltzer, N., Lalaoui, N., Lawlor, K. E., Vanyai, H., Hall, C., Bankovacki, A., Gangoda, L., Wong, W. W., Corbin, J., Huang, C., Mocarski, E. S., Murphy, J. M., Alexander, W. S., Voss, A. K., Vaux, D. L., Kaiser, W. J., Walczak, H. and Silke, J. (2014) TNFR1-dependent cell death drives inflammation in Sharpin-deficient mice. *Elife.* **3**
- 4 Dillon, C. P., Weinlich, R., Rodriguez, D. A., Cripps, J. G., Quarato, G., Gurung, P., Verbist, K. C., Brewer, T. L., Llambi, F., Gong, Y. N., Janke, L. J., Kelliher, M. A., Kanneganti, T. D. and Green, D. R. (2014) RIPK1 blocks early postnatal lethality mediated by caspase-8 and RIPK3. *Cell.* **157**, 1189-1202
- 5 Kaiser, W. J., Daley-Bauer, L. P., Thapa, R. J., Mandal, P., Berger, S. B., Huang, C., Sundararajan, A., Guo, H., Roback, L., Speck, S. H., Bertin, J., Gough, P. J., Balachandran, S. and Mocarski, E. S. (2014) RIP1 suppresses innate immune necrotic as well as apoptotic cell death during mammalian parturition. *Proc Natl Acad Sci U S A.* **111**, 7753-7758
- 6 Takahashi, N., Vereecke, L., Bertrand, M. J., Duprez, L., Berger, S. B., Divert, T., Goncalves, A., Sze, M., Gilbert, B., Kourula, S., Goossens, V., Lefebvre, S., Gunther, C., Becker, C., Bertin, J., Gough, P. J., Declercq, W., van Loo, G. and Vandenabeele, P. (2014) RIPK1 ensures intestinal homeostasis by protecting the epithelium against apoptosis. *Nature.* **513**, 95-99
- 7 Dannappel, M., Vlantis, K., Kumari, S., Polykratis, A., Kim, C., Wachsmuth, L., Eftychi, C., Lin, J., Corona, T., Hermance, N., Zelic, M., Kirsch, P., Basic, M., Bleich, A., Kelliher, M. and Pasparakis, M. (2014) RIPK1 maintains epithelial homeostasis by inhibiting apoptosis and necroptosis. *Nature.* **513**, 90-94
- 8 Pasparakis, M. and Vandenabeele, P. (2015) Necroptosis and its role in inflammation. *Nature.* **517**, 311-320
- 9 Wu, J., Huang, Z., Ren, J., Zhang, Z., He, P., Li, Y., Ma, J., Chen, W., Zhang, Y., Zhou, X., Yang, Z., Wu, S. Q., Chen, L. and Han, J. (2013) Mlkl knockout mice demonstrate the indispensable role of Mlkl in necroptosis. *Cell Res.* **23**, 994-1006
- 10 He, S., Wang, L., Miao, L., Wang, T., Du, F., Zhao, L. and Wang, X. (2009) Receptor interacting protein kinase-3 determines cellular necrotic response to TNF-alpha. *Cell.* **137**, 1100-1111
- 11 Duprez, L., Takahashi, N., Van Hauwermeiren, F., Vandendriessche, B., Goossens, V., Vanden Berghe, T., Declercq, W., Libert, C., Cauwels, A. and Vandenabeele, P. (2011) RIP kinase-dependent necrosis drives lethal systemic inflammatory response syndrome. *Immunity.* **35**, 908-918
- 12 Cho, Y. S., Challa, S., Moquin, D., Genga, R., Ray, T. D., Guildford, M. and Chan, F. K. (2009) Phosphorylation-driven assembly of the RIP1-RIP3 complex regulates programmed necrosis and virus-induced inflammation. *Cell.* **137**, 1112-1123

- 13 Moujalled, D. M., Cook, W. D., Okamoto, T., Murphy, J., Lawlor, K. E., Vince, J. E. and Vaux, D. L. (2013) TNF can activate RIPK3 and cause programmed necrosis in the absence of RIPK1. *Cell Death Dis.* **4**, e465
- 14 Khan, N., Lawlor, K. E., Murphy, J. M. and Vince, J. E. (2014) More to life than death: molecular determinants of necroptotic and non-necroptotic RIP3 kinase signaling. *Curr Opin Immunol.* **26**, 76-89
- 15 Sun, L., Wang, H., Wang, Z., He, S., Chen, S., Liao, D., Wang, L., Yan, J., Liu, W., Lei, X. and Wang, X. (2012) Mixed lineage kinase domain-like protein mediates necrosis signaling downstream of RIP3 kinase. *Cell.* **148**, 213-227
- 16 Zhao, J., Jitkaew, S., Cai, Z., Choksi, S., Li, Q., Luo, J. and Liu, Z. G. (2012) Mixed lineage kinase domain-like is a key receptor interacting protein 3 downstream component of TNF-induced necrosis. *Proc Natl Acad Sci U S A.* **109**, 5322-5327
- 17 Murphy, J. M., Czabotar, P. E., Hildebrand, J. M., Lucet, I. S., Zhang, J. G., Alvarez-Diaz, S., Lewis, R., Lalaoui, N., Metcalf, D., Webb, A. I., Young, S. N., Varghese, L. N., Tannahill, G. M., Hatchell, E. C., Majewski, I. J., Okamoto, T., Dobson, R. C. J., Hilton, D. J., Babon, J. J., Nicola, N. A., Strasser, A., Silke, J. and Alexander, W. S. (2013) The pseudokinase MLKL mediates necroptosis via a molecular switch mechanism. *Immunity.* **39**, 443-453
- 18 Murphy, J. M., Zhang, Q., Young, S. N., Reese, M. L., Bailey, F. P., Eyers, P. A., Ungureanu, D., Hammaren, H., Silvennoinen, O., Varghese, L. N., Chen, K., Tripaydonis, A., Jura, N., Fukuda, K., Qin, J., Nimchuk, Z., Mudgett, M. B., Elowe, S., Gee, C. L., Liu, L., Daly, R. J., Manning, G., Babon, J. J. and Lucet, I. S. (2014) A robust methodology to subclassify pseudokinases based on their nucleotide-binding properties. *Biochem J.* **457**, 323-334
- 19 Murphy, J. M., Lucet, I. S., Hildebrand, J. M., Tanzer, M. C., Young, S. N., Sharma, P., Lessene, G., Alexander, W. S., Babon, J. J., Silke, J. and Czabotar, P. E. (2014) Insights into the evolution of divergent nucleotide-binding mechanisms among pseudokinases revealed by crystal structures of human and mouse MLKL. *Biochem J.* **457**, 369-377
- 20 Hildebrand, J. M., Tanzer, M. C., Lucet, I. S., Young, S. N., Spall, S. K., Sharma, P., Pierotti, C., Garnier, J. M., Dobson, R. C., Webb, A. I., Tripaydonis, A., Babon, J. J., Mulcair, M. D., Scanlon, M. J., Alexander, W. S., Wilks, A. F., Czabotar, P. E., Lessene, G., Murphy, J. M. and Silke, J. (2014) Activation of the pseudokinase MLKL unleashes the four-helix bundle domain to induce membrane localization and necroptotic cell death. *Proc Natl Acad Sci U S A.* **111**, 15072-15077
- 21 Dondelinger, Y., Declercq, W., Montessuit, S., Roelandt, R., Goncalves, A., Bruggeman, I., Hulpiau, P., Weber, K., Schon, C. A., Marquis, R. W., Bertin, J., Gough, P. J., Savvides, S., Martinou, J. C., Bertrand, M. J. and Vandenabeele, P. (2014) MLKL compromises plasma membrane integrity by binding to phosphatidylinositol phosphates. *Cell Rep.* **7**, 971-981
- 22 Chen, X., Li, W., Ren, J., Huang, D., He, W. T., Song, Y., Yang, C., Li, W., Zheng, X., Chen, P. and Han, J. (2014) Translocation of mixed lineage kinase domain-like protein to plasma membrane leads to necrotic cell death. *Cell Res.* **24**, 105-121
- 23 Wang, H., Sun, L., Su, L., Rizo, J., Liu, L., Wang, L. F., Wang, F. S. and Wang, X. (2014) Mixed Lineage Kinase Domain-like Protein MLKL Causes Necrotic Membrane Disruption upon Phosphorylation by RIP3. *Mol Cell.* **54**, 133-146
- 24 Cai, Z., Jitkaew, S., Zhao, J., Chiang, H. C., Choksi, S., Liu, J., Ward, Y., Wu, L. G. and Liu, Z. G. (2014) Plasma membrane translocation of trimerized MLKL protein is required for TNF-induced necroptosis. *Nat Cell Biol.* **16**, 55-65

- 25 Cook, W. D., Moujalied, D. M., Ralph, T. J., Lock, P., Young, S. N., Murphy, J. M. and Vaux, D. L. (2014) RIPK1- and RIPK3-induced cell death mode is determined by target availability. *Cell Death Differ.* **21**, 1600-1612
- 26 Dephoure, N., Zhou, C., Villen, J., Beausoleil, S. A., Bakalarski, C. E., Elledge, S. J. and Gygi, S. P. (2008) A quantitative atlas of mitotic phosphorylation. *Proc Natl Acad Sci U S A.* **105**, 10762-10767
- 27 Daub, H., Olsen, J. V., Bairlein, M., Gnad, F., Oppermann, F. S., Korner, R., Greff, Z., Keri, G., Stemmann, O. and Mann, M. (2008) Kinase-selective enrichment enables quantitative phosphoproteomics of the kinome across the cell cycle. *Mol Cell.* **31**, 438-448
- 28 Xie, T., Peng, W., Yan, C., Wu, J., Gong, X. and Shi, Y. (2013) Structural Insights into RIP3-Mediated Necroptotic Signaling. *Cell Rep.* **5**, 70-78
- 29 Newton, K., Sun, X. and Dixit, V. M. (2004) Kinase RIP3 is dispensable for normal NF-kappa Bs, signaling by the B-cell and T-cell receptors, tumor necrosis factor receptor 1, and Toll-like receptors 2 and 4. *Mol Cell Biol.* **24**, 1464-1469
- 30 Verhagen, A. M., Ekert, P. G., Pakusch, M., Silke, J., Connolly, L. M., Reid, G. E., Moritz, R. L., Simpson, R. J. and Vaux, D. L. (2000) Identification of DIABLO, a mammalian protein that promotes apoptosis by binding to and antagonizing IAP proteins. *Cell.* **102**, 43-53
- 31 Wisniewski, J. R., Zougman, A., Nagaraj, N. and Mann, M. (2009) Universal sample preparation method for proteome analysis. *Nat Methods.* **6**, 359-362
- 32 Cox, J., Neuhauser, N., Michalski, A., Scheltema, R. A., Olsen, J. V. and Mann, M. (2011) Andromeda: a peptide search engine integrated into the MaxQuant environment. *J Proteome Res.* **10**, 1794-1805
- 33 Rodriguez, D. A., Weinlich, R., Brown, S., Guy, C., Fitzgerald, P., Dillon, C. P., Oberst, A., Quarato, G., Low, J., Cripps, J. G., Chen, T. and Green, D. R. (2015) Characterization of RIPK3-mediated phosphorylation of the activation loop of MLKL during necroptosis. *Cell Death Differ.* **In press**

## FIGURE LEGENDS

### Figure 1: Cell death occurs much later than MLKL activation loop phosphorylation following TSQ stimulation.

U937 (A) and HT29 (C) were left untreated or treated with TSQ (100 ng/ml TNF, 500 nM Smac-mimetic, 10  $\mu$ M Q-VD-OPh) for 3, 6, 10, 24, 48 hours. Phosphorylated MLKL and total MLKL levels were determined by immunoblotting, and the actin immunoblot served as a loading control. In parallel to the experiments shown in panels A and C, U937 (B) and HT29 (D) were treated as above and cell death analysed by Propidium Iodide (PI) staining and flow cytometry. Data are plotted as mean  $\pm$  SEM for three independent experiments. (E) Cytoplasmic (“C”) and membrane fractions (“M”) of lysates from U937 cells treated for 3, 6, 10, 24 hours with TSQ were separated on Blue-Native PAGE and analysed with phospho-MLKL and total MLKL antibodies. The asterisk corresponds to a band arising from cross-reactivity of the anti-phosphoMLKL antibody with a component of the molecular weight marker. Anti-GAPDH and anti-VDAC blots were performed to determine the fractionation purity and protein abundance in the cytoplasmic and membrane fractions, respectively. The low and high molecular weight MLKL-containing complexes are respectively termed “I” and “II”, as previously [20]. Data presented in panels A, C are representative of three independent experiments and panel E representative of two independent experiments.

### Figure 2: Identification of three novel phosphorylation sites of MLKL using mass spectrometry.

(A) The crystal structure of full length mouse MLKL (PDB, 4BTF; [17]) annotated with sites of phosphorylation. S345, S347 and T349 were reported in references [17, 28]; S124 is the mouse counterpart of a human MLKL phosphosite reported in [26, 27]; S158, S228 and S248 were identified in the present study.

(B-D) Mass spectra from which S228, S248 and S158 in mouse MLKL were identified as phosphosites. Fragment ions ( $y$  ions = red ticks and  $b$  ions = blue ticks) containing the neutral loss of phosphate are marked by asterisks.

### Figure 3: Phospho-ablating and phospho-mimetic sites of MLKL have different effects on cell death.

(A-J) Biologically independent MDF cell lines derived from three wild-type (*wt*) or three *Mlkl*<sup>-/-</sup> mice were stably infected with doxycycline inducible constructs encoding full-length MLKL harbouring different phospho-ablating and phospho-mimetic mutations. Expression of mutants was induced for 4 hours with 10 ng/ml doxycycline (black bars for *wt*, grey bars for *Mlkl*<sup>-/-</sup>) or not (white bars) before induction of apoptosis with TS and necroptosis with TSQ for 24 hours. Cell death was analysed by detecting PI-permeable cells using flow cytometry. Data are plotted as mean  $\pm$  SEM, n=6; 3 biological samples assayed twice.

### Figure 4: Activated MLKL mutants induce cell death independently of endogenous RIPK3 and MLKL.

(A) The levels of endogenous MLKL and RIPK3 proteins in wild-type, *Mlkl*<sup>-/-</sup> and *Ripk3*<sup>-/-</sup>*Mlkl*<sup>-/-</sup> cells was assessed by immunoblotting in three biologically independent cell lines for each genotype. (B) Wild-type, *Mlkl*<sup>-/-</sup> and *Ripk3*<sup>-/-</sup>*Mlkl*<sup>-/-</sup> cells were untreated, or treated with the apoptotic stimulus (TS) or the necroptotic stimulus (TSQ) for 24 hours and cell death was enumerated by flow cytometry of PI-permeable cells. (C-L) *Ripk3*<sup>-/-</sup>*Mlkl*<sup>-/-</sup> MDFs were stably infected with doxycycline-inducible MLKL mutants and assayed in two independent experiments. Cell lines were induced with 10 ng/ml doxycycline (white bars) or not (grey bars) followed by treatment with the apoptosis stimulus (TS) and necroptotic

stimulus (TSQ) for 24 hours. PI-permeable cells were quantified using flow cytometry. Data of three or more biological replicates assayed twice are plotted as mean  $\pm$  SEM, n=6; 3 biological samples assayed twice.

**Figure 5: Auto-activated MLKL mutants translocate to the membrane independently of RIPK3.**

(A) Membrane translocation and high molecular weight complex formation by the auto-activating MLKL mutant (S345D) was examined by Blue-Native PAGE in wild-type (*wt*), *Mlkl*<sup>-/-</sup> and *Ripk3*<sup>-/-</sup>*Mlkl*<sup>-/-</sup> MDF cells 7.5 hours post-induction of expression with doxycycline (Dox). Cells were fractionated into cytoplasmic (“C”) and membrane (“M”) fractions and proteins resolved by Blue-Native PAGE. Localisation of endogenous MLKL was examined in wild-type MDFs that were untreated (UT) or treated with TSQ for 7.5 hours (left lanes). The low and high molecular weight MLKL-containing complexes are termed “I” and “II”, as previously [20].

(B, C) Cytoplasmic and membrane fractions of phospho-ablating and phospho-mimetic MLKL mutants inducibly-expressed in *Ripk3*<sup>-/-</sup>*Mlkl*<sup>-/-</sup> MDFs for 7 hours with doxycycline (Dox) were examined by Blue-Native PAGE. Membrane fractionation purity and protein abundance was assessed by immunoblotting for GAPDH and VDAC, markers of cytoplasmic and membrane fractions, respectively. Migration of molecular weight standards (kDa) are shown on the right of blots. Migration of low (“I”) and high (“II”) molecular weight species are marked on the left of the Blue-Native PAGE. Data in each panel are representative of two independent experiments.

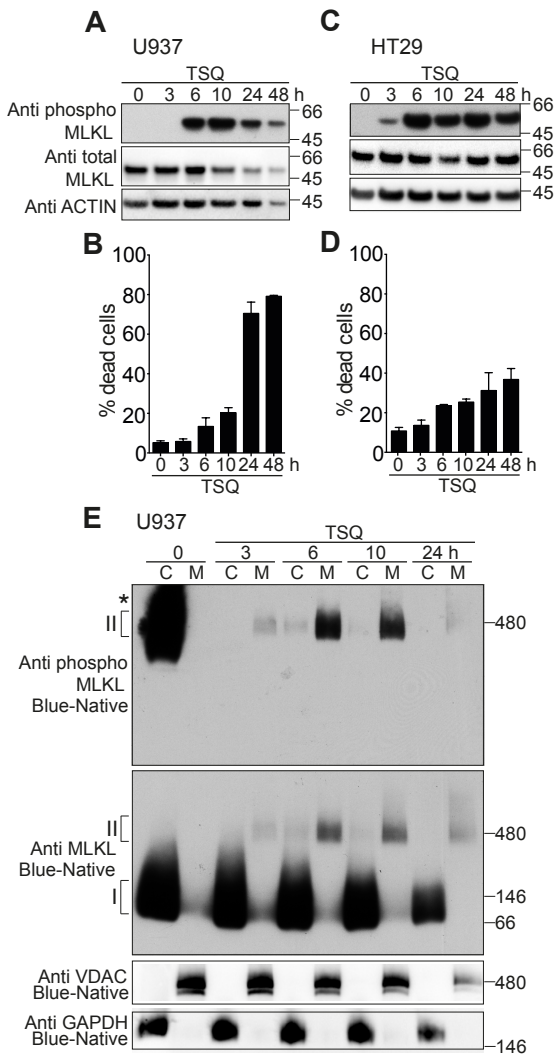
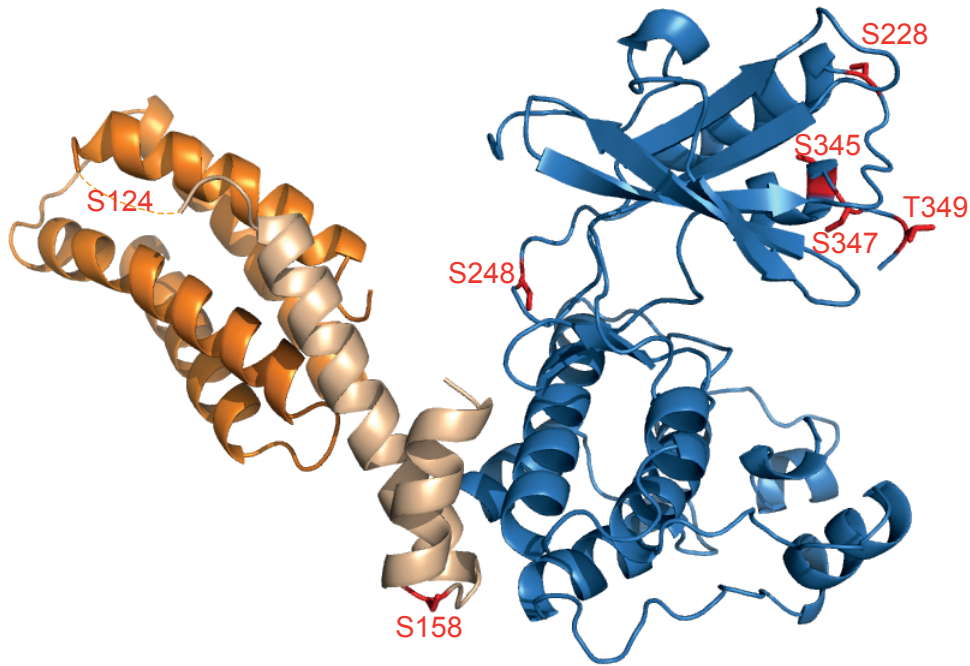
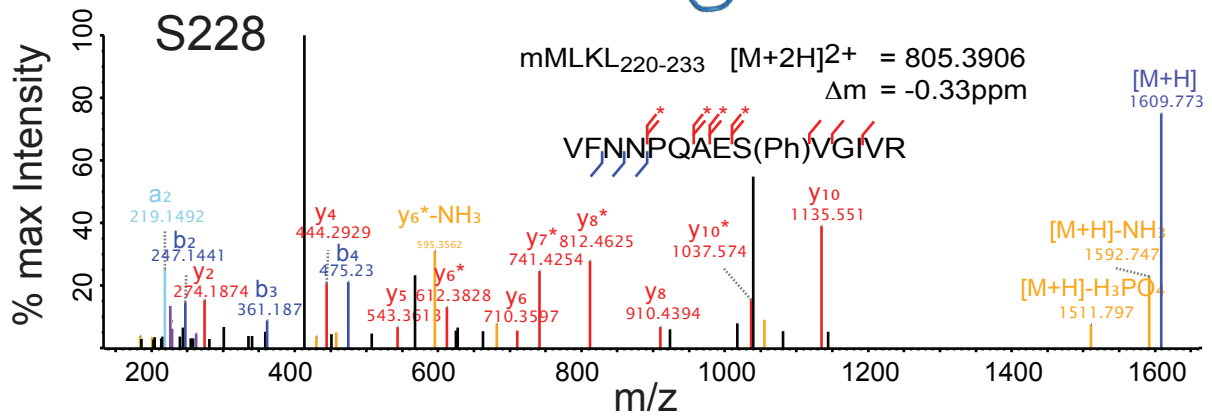


Figure 1

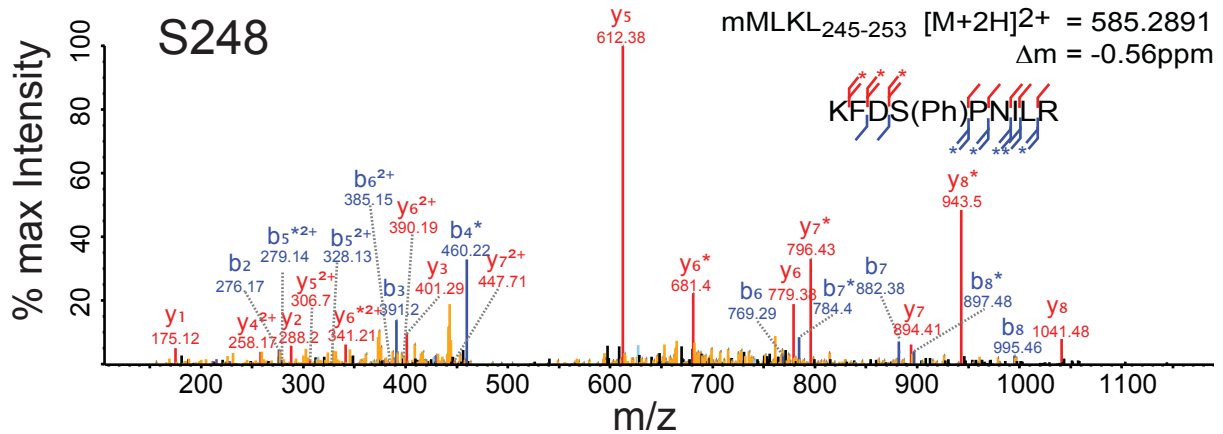
A



B



C



D

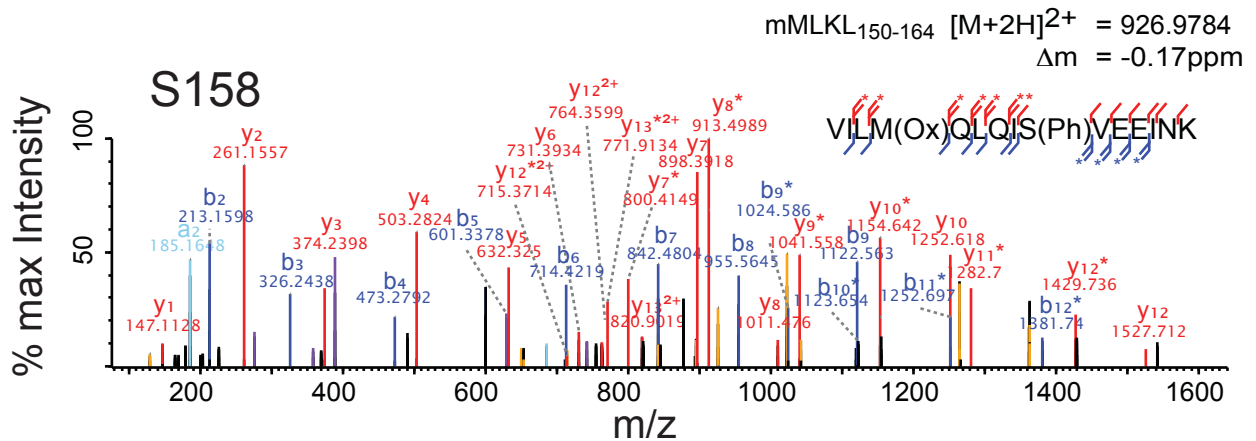


Figure 2

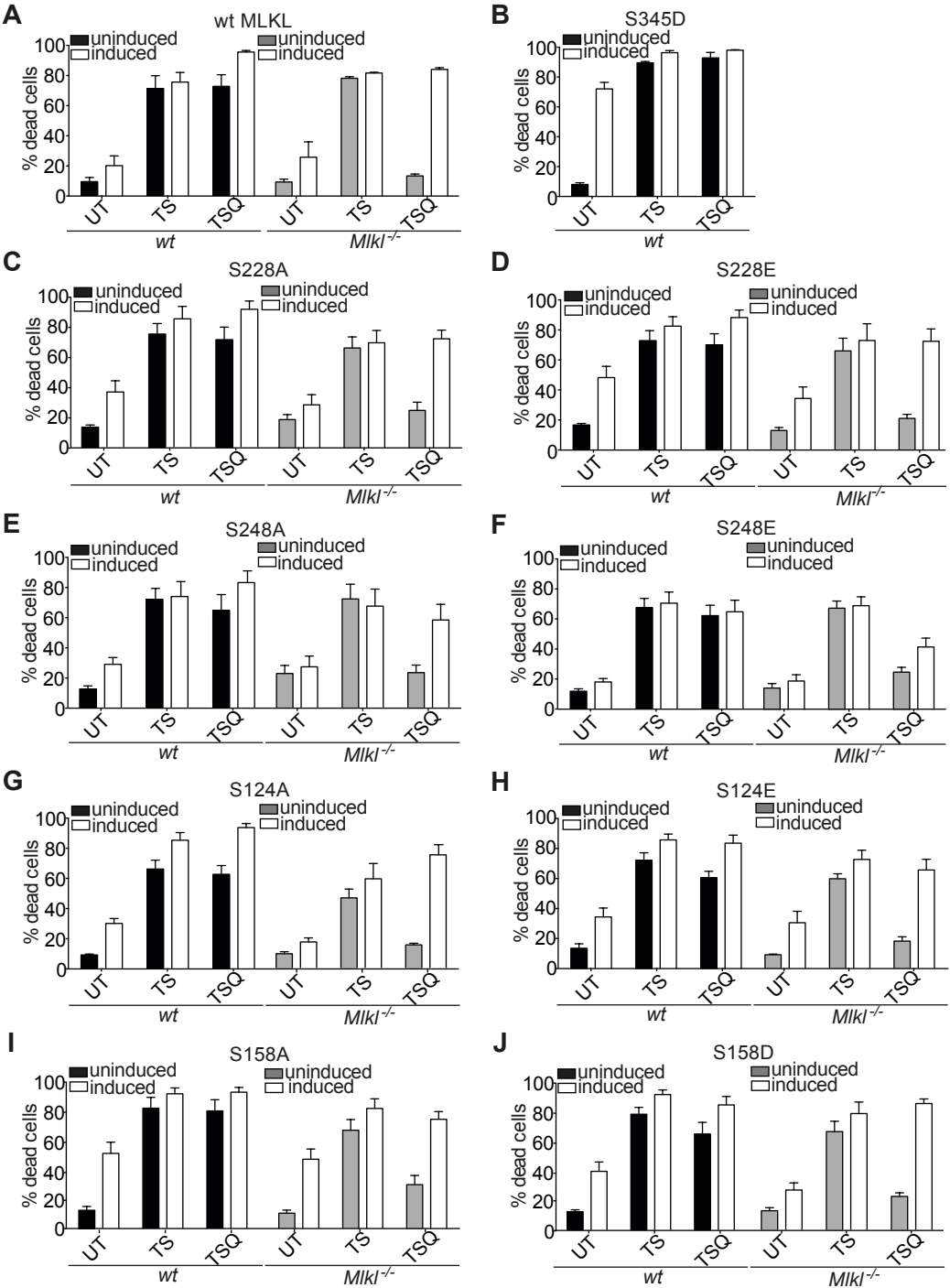


Figure 3

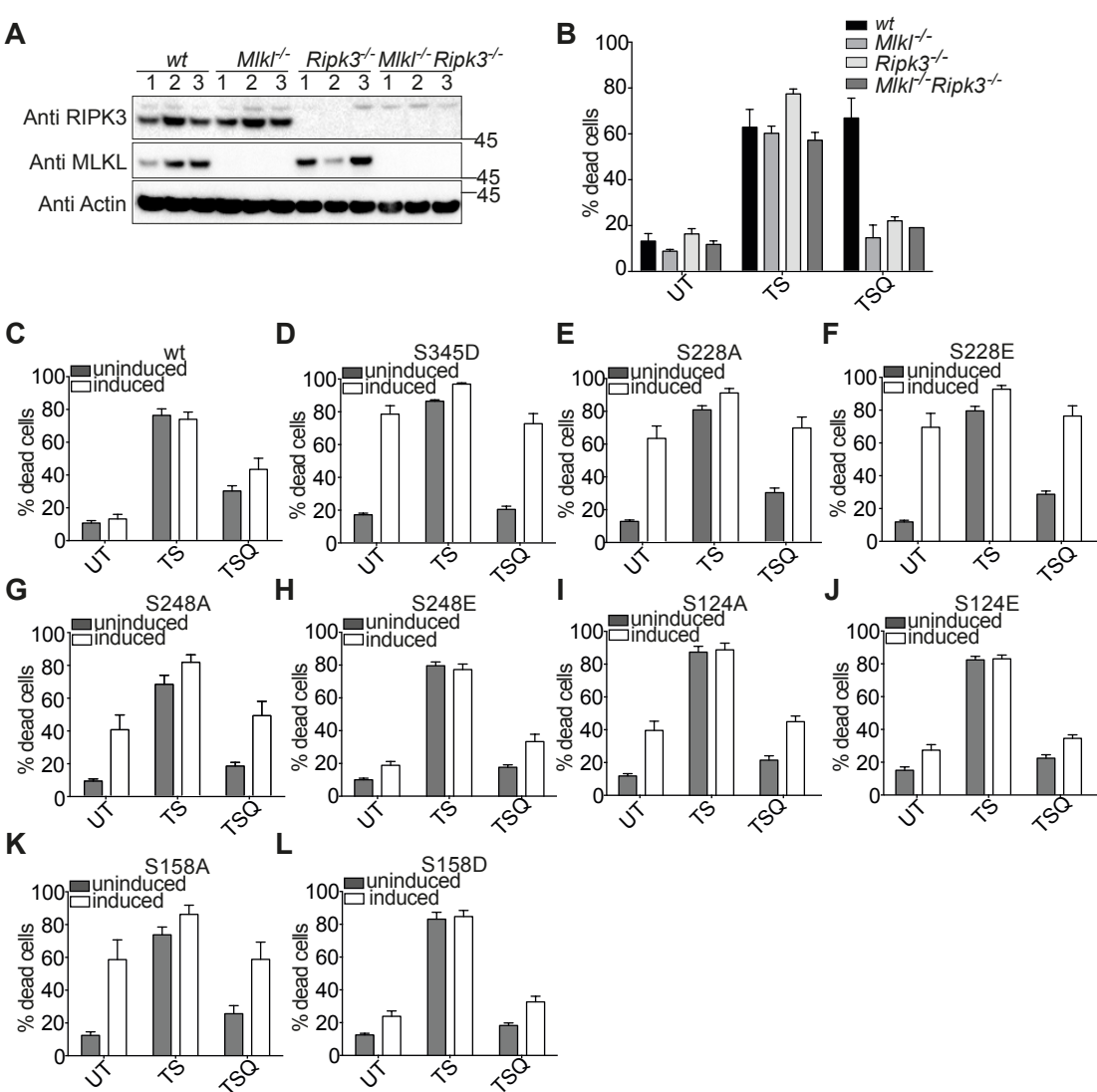


Figure 4

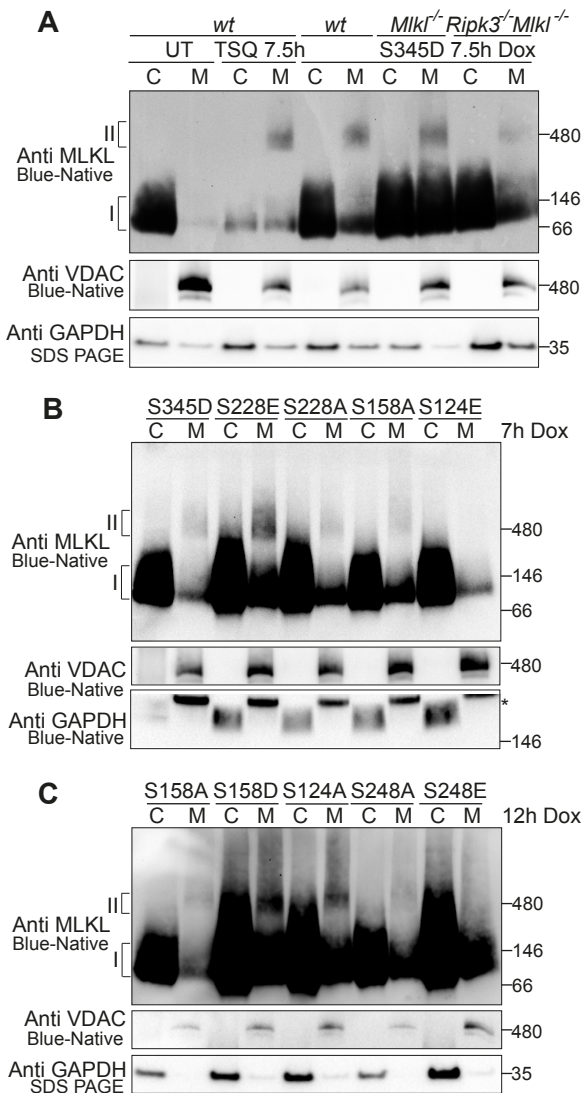


Figure 5